

Chemical tagging of stellar kinematic groups

H.M. Taberero¹, D. Montes¹, and J.I. González Hernández^{2,3}

¹ Dpto. de Astrofísica, Facultad de CC. Físicas, Universidad Complutense de Madrid, E-28040 Madrid, Spain

² Instituto de Astrofísica de Canarias, Cl. Via Lactea s/n, E-38200 La Laguna, Tenerife, Spain

³ Dept. Astrofísica, Universidad de La Laguna (ULL), E-38206 La Laguna, Tenerife, Spain

Abstract

Stellar Kinematic Groups are kinematical coherent groups of stars which might share a common origin. These groups spread through the Galaxy over time due to tidal effects caused by galactic rotation and disc heating, however the chemical information survives. The aim of chemical tagging is to show that abundances of every chemical element must be homogeneous among candidate members. We have studied the case of the Hyades Supercluster and the Ursa Major Moving Group for kinematically selected FGK stars, based on high-resolution spectroscopic observations obtained at the 1.2 m Mercator Telescope with the HERMESSpectrograph. Stellar atmospheric parameters (T_{eff} , $\log g$, ξ and $[\text{Fe}/\text{H}]$) have been determined using an own-implemented automatic code (STEPAR) which makes use of the sensibility from iron EWs measured in the spectra. We have derived the chemical abundances of several elements and their $[\text{X}/\text{Fe}]$ ratios. Thus, we finally perform a careful differential abundance analysis using a known member of each cluster as a reference star, with the aim to clarify the origin of these kinematical groups.

1 Introduction

Stellar kinematic groups (SKGs) –superclusters (SCs) and moving groups (MGs)– are kinematic coherent groups of stars [10] that could share a common origin. The youngest and most well-studied SKGs are: the Hyades SC (600 Myr), the Ursa Major MG (Sirius SC, 300 Myr), the Local Association or Pleiades MG (20 to 150 Myr), the IC 2391 SC (35-55 Myr), and the Castor MG (200 Myr) [20]. Olin Eggen introduced the concept of MG and the fact that stars can maintain a kinematic signature over long periods of time. However, their existence has been disputed, specially in the case of the Old MGs. There are two factors that

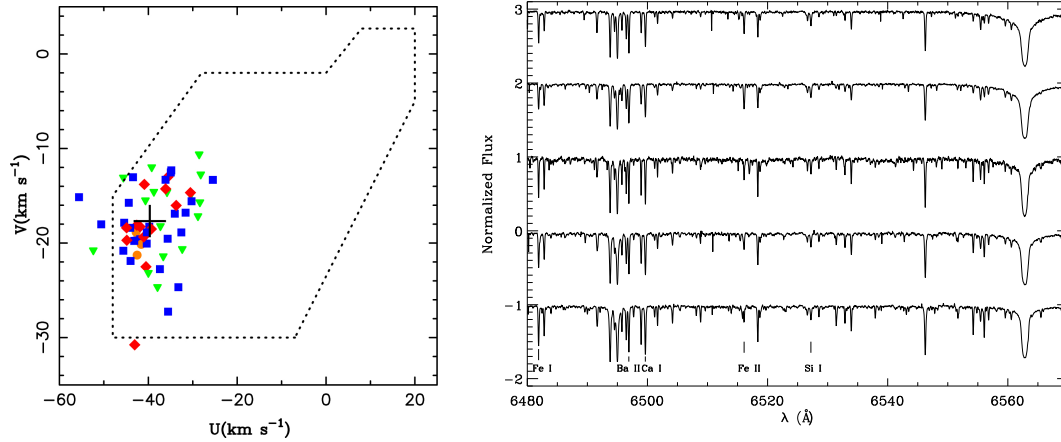


Figure 1: *Left panel:* U and V velocities for the possible members of the Hyades Supercluster. Blue squares represent stars selected as members by the *chemical tagging* approach, red diamonds represent stars that have similar Fe abundances, but not for all the elements. Orange circles represent three Hyades cluster stars (BZ Cet, V683 Per, and ϵ Tau). Green triangles represent stars that do have similar Fe abundances (as well as similar values of other elements). The big black cross indicates the U , V , and W central location of the Hyades Supercluster (see [20]). Dashed lines show the region where the majority of the young disk stars tend to be according to [10]. *Right panel:* High resolution spectra for some representative stars from our sample (from top to bottom), HD 27285 (G4 V), HD 53532 (G3 V), HD 98356 (K0 V), these three stars satisfy *chemical tagging* membership conditions, vB 153 (a K0 V reference star used in the differential abundances analysis) and BZ Cet (a K2 V, also member of the Hyades cluster). Lines used in the abundance analysis are highlighted on bottom.

can disrupt a MG: the Galactic differential rotation which tends to disperse the stars, and the disc heating, which causes velocity the dispersion of the disc stars to increase with age.

However, the detailed analysis of the chemical content (*chemical tagging*) is another powerful method that provide clear constraints on membership to these structures (see [12]). Studies of open clusters, such as the Hyades and Collinder 261 [23, 5, 6, 8] have found high levels of chemical homogeneity, showing that chemical information is preserved within their original stars. Also possible effects of any external sources of pollution during the evolution of the stars are negligible. *Chemical tagging* has been applied also to three old MGs: The Hercules Stream [2], HR 1614 [7, 8] and Wolf 630 [3]. The last two appear to be true MGs. In addition, only two young moving groups have been studied under the *chemical tagging* approach: the Hyades Supercluster, which can not be originated entirely from the Hyades cluster [25, 9, 30], and the Ursa Major Moving Group, consistent with a true MG of $[\text{Fe}/\text{H}] = -0.085$ (see [1, 32, 33]). We will concentrate here on the results concerning the Hyades Supercluster (for further details see [30]).

2 Sample selection

The sample stars analyzed were selected using kinematical criteria based on their U , V and W Galactic velocities. We allowed stars to become candidate members if they were within approximately 10 km s^{-1} of the mean velocity of the group (see [20, 16, 19, 18, 21]). After the first stage of selection based on kinematical criteria, we then eliminated stars that were unsuitable for our particular spectroscopic analysis: Stars hotter than F6 and Cooler than K4, fast rotators ($v \sin i \geq 15 \text{ km s}^{-1}$) and well-known doubled line spectroscopic binaries. We recalculated the Galactic velocities of our selected targets by employing the radial velocities and uncertainties derived by the HERMES spectrograph automated pipeline [26]. Proper motions and parallaxes were taken from the *Hipparcos* and Tycho catalogues [11], the Tycho-2 catalogue [14], and the new reduction of the *Hipparcos* catalogue [17]. We employ the approach of [20] to perform the Galactic-velocity calculation and associated errors. The obtained velocities are represented in Fig. 1.

3 Observations

Spectroscopic observations (see Fig. 1) were obtained at the 1.2 m Mercator Telescope at the Observatorio del Roque de los Muchachos (La Palma, Spain) in January, May, and November 2010 with HERMES (High Efficiency and Resolution Mercator Echelle Spectrograph, see [26]). Using the high resolution mode (HRF), the spectral resolution is 85000 and the wavelength range is from $\lambda 3800 \text{ \AA}$ to $\lambda 8750 \text{ \AA}$ approximately. Our signal-to-noise ratio (S/N) ranges from 70 to 300 (160 on average) in the V band. A total of 92 stars were observed. We analyzed single main-sequence and giant stars (from F6 to K4), including 61 candidates in total and the Hyades Cluster reference star vB 153 (as in [23]). All the obtained *echelle* spectra were reduced with the automatic pipeline [26] for HERMES. We later used several IRAF¹ tasks to normalize the spectra order by order, using a low-order polynomial fit to the observed continuum, merging the orders into a unique one-dimensional spectrum and applying the Doppler correction required for its observed radial velocity.

4 Stellar Parameters

Stellar atmospheric parameters and abundances were computed using the 2002 version of the MOOG code [27] and a grid of Kurucz ATLAS9 plane-parallel model atmospheres [15]. The atmospheric parameters were inferred from 263 Fe I and 36 Fe II lines (the iron lines and their atomic parameters were obtained from [29]) iterating until the slopes of χ versus (vs.) $\log \epsilon(\text{Fe I})$ and $\log(EW/\lambda)$ vs. $\log \epsilon(\text{Fe I})$ were zero (excitation equilibrium) and imposing ionization equilibrium, such that $\log \epsilon(\text{Fe I}) = \log \epsilon(\text{Fe II})$. To simplify the iterative procedure, we built an automatic code called STEPAR (see [30, 31]), that employs a Downhill Simplex Method [24], this code finds the best solution in the parameter space within minutes.

¹IRAF is distributed by the National Optical Observatory, which is operated by the Association of Universities for Research in Astronomy, Inc., under contract with the National Science Foundation.

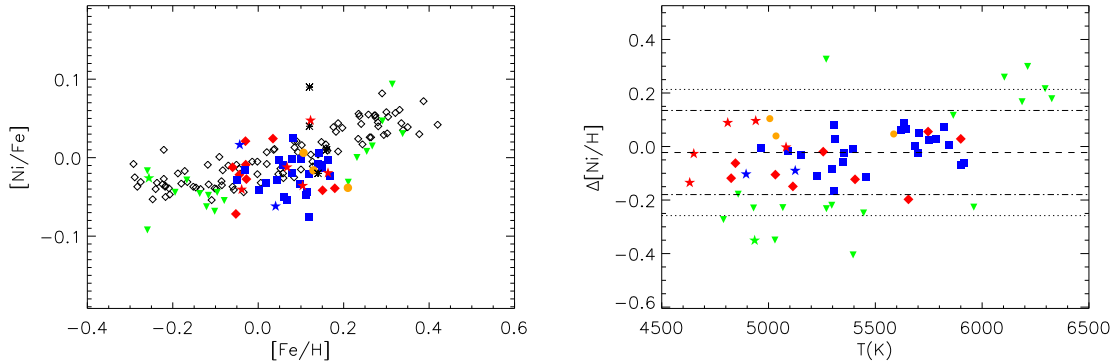


Figure 2: *Right panel:* $[\text{Ni}/\text{Fe}]$ vs. $[\text{Fe}/\text{H}]$ open diamonds represent the thin disc data [13], black upward-pointing filled triangles represent Hyades cluster data [23], red diamonds are our stars compatible to within 1-rms with the Fe abundance but not for all elements, blue squares and blue starred symbols are the candidates selected to become members of the Hyades Supercluster. Green downward-pointing triangles show no compatible stars. BZ Cet, V683 Per, and ϵ Tau Hyades cluster members stars are marked with orange circles. Starred points represent the giant stars. Black asterisks are the candidates selected by [9] and black crosses represent the members selected by [25]. *Left panel:* Same as left panel but for $\Delta[\text{Ni}/\text{H}]$ vs T_{eff}

The obtained solution for a given star is independent of the initial set of parameters employed, hence we used the canonical solar values as initial input values ($T_{\text{eff}}=5777$ K, $\log g=4.44$ dex, $\xi=1$ km s^{-1}).

The *EW* determination of the Fe lines was carried out with the ARES² code [28]. We followed the approach of [29] to adjust the *rejt* parameter of ARES according to the *S/N* of each spectrum. The other ARES parameters we employed were *smoother* = 4, *space* = 3, *lineresol* = 0.07, and *miniline* = 2. In addition, we performed a $2\text{-}\sigma$ rejection of the Fe I-II lines after a first determination of the stellar parameters, therefore we re-run the STEPAR program again without the rejected lines. As a test, we performed the parameter determination in the case of the Sun. Employing a HERMES spectrum of the asteroid Vesta with the same instrumental configuration as the other stars. In this case, we obtained: $T_{\text{eff}} = 5775 \pm 15$ (K), $\log g = 4.48 \pm 0.04$ (dex), $\xi = 0.965 \pm 0.020$ (km s^{-1}), and $\log \epsilon(\text{Fe I}) = 7.46 \pm 0.01$ (dex), which are very close to the canonical solar values of the atmospheric parameters.

5 Elemental abundances

The selection of the chemical elements that we considered in this study includes those in the line list of [22], which also provides the atomic parameters for each line. In addition, we considered some lines from [13, 25] of some neutron-capture elements, treating 20 different

²The ARES code can be downloaded at <http://www.astro.up.pt/>

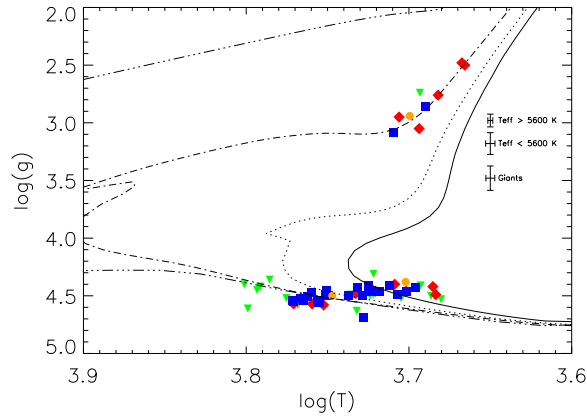


Figure 3: Spectroscopic $\log T_{\text{eff}}$ vs. $\log g$ for the candidate stars. We have employed the Yonsei-Yale isochrones [4] for $Z = 0.025$ and 0.1, 0.7, 4, and 13 Gyr (from left to right). Mean error bars are represented at the middle right. Blue squares represent stars selected as members by the *chemical tagging* approach, red diamonds represent those stars that have similar Fe abundances, but different values of other elements. Orange circles represent three Hyades cluster stars (BZ Cet, V683 Per and ϵ Tau). Green triangles represent those stars that do not have similar Fe abundances (as well as dissimilar values of other elements).

chemical elements in total (Fe, Na, Mg, Al, Si, Ca, Ti, V, Cr, Mn, Co, Fe, Ni, Cu, Zn, Y, Zr, Ba, Ce, and Nd). The EW determination is the same as stated in Section 4, the abundances from each line are determined with the MOOG code [27]. We also obtained differential abundances $\Delta[X/H]$ by comparing with a reference star known to be a member of the Hyades cluster (vB 153) on a line-by-line basis. The candidate selection within the sample was determined by applying a one root-mean-squared (rms, thereafter) rejection over the median for almost every chemical element treated in the analysis. The rejection process considers the rms in the abundances of the sample for each element. At first, we rejected every star that deviated by more than 1-rms from the median abundance denoted by the dashed-dotted lines in Fig. 2. The initial 1-rms rejections led to the identification of 15 candidate members (a 25 % of the sample). We subsequently applied a more flexible criteria allowing stars to become members when their abundances were within the 1-rms interval for 90 % of the elements considered and the remaining 10 % within the 1.5-rms interval (18 elements and 2 elements respectively). This more flexible rms-based analysis was made in order to see to the degree which the sample is homogeneous, and to take care of the more likely contamination of the sample by field stars. Hence, allowing two elements (maximum) to satisfy the 1.5-rms criteria results in 28 candidate members (46 %). Adopting these criteria, we conclude that the membership of the Hyades Supercluster ranges from 25 to 46 %.

6 Conclusions

The abundance analysis shows that the final 28 selected stars are compatible with the Hyades isochrone (see Fig. 3), as expected if they have evaporated from the Hyades cluster. Our analysis does not recover the same number of members as the two previous studies of [25] and [9]. The abundance selection in the case of [25] is based on a statistical contrast based on a χ^2 test that employs a few Hyades Cluster stars. This χ^2 approach treats all the abundances as whole, thus does not concentrate on the individual elements one by one. On the other hand, [9] discard the stars for which the Fe abundances are lower than the solar value. They identified a few stars that might have originated from the original cluster based on this Fe preselection. Later on, they analyzed the trends of other elements to determine whether these stars have the same abundance as the Hyades Cluster. All these samples are incomplete but no robust assesment of the contamination levels of the Hyades Supercluster can be made. The method used in the present study (as in [25, 9]) can only ascertain the origin of the Hyades Supercluster but cannot measure the contamination levels by field stars. The common conclusion of this work and [25, 9] is that the Hyades Supercluster cannot originate entirely from the Hyades Cluster. However, we can still identify candidates that once belonged to the Hyades cluster.

Acknowledgments

This work was supported by the Universidad Complutense de Madrid (UCM), the Spanish Ministerio de Economía y Competitividad (MINECO) under grants BES-2009-012182, and AYA2011-30147-C03-02, and The Comunidad de Madrid under PRICIT project S2009/ESP-1496 (AstroMadrid).

References

- [1] Ammler-von Eiff, M. & Guenther, E. W. 2009, *A&A*, 508, 677
- [2] Bensby, T., Oey, M. S., Feltzing, S., & Gustafsson, B. 2007, *ApJ*, 655, L89
- [3] Bubar, E. J. & King, J. R. 2010, *AJ*, 140, 293
- [4] Demarque, P., Woo, J.-H., Kim, Y.-C., & Yi, S. K. 2004, *ApJs*, 155, 667
- [5] De Silva, G. M., Sneden, C., Paulson, D. B., et al. 2006, *AJ*, 131, 455
- [6] De Silva, G. M., Freeman, K. C., Asplund, M., et al. 2007, *AJ*, 133, 1161
- [7] De Silva, G. M., Freeman, K. C., Bland-Hawthorn, J., et al. 2007, *AJ*, 133, 694
- [8] De Silva, G. M., Freeman, K. C., & Bland-Hawthorn, J. 2009, *PASA*, 26, 11
- [9] De Silva, G. M., Freeman, K. C., Bland-Hawthorn, J., et al. 2011, *MNRAS*, 415, 563
- [10] Eggen, O. J. 1994, *Galactic and Solar System Optical Astrometry*, 191

- [11] ESA, 1997, *The Hipparcos and Tycho Catalogues*, ESA SP-1200
- [12] Freeman, K. & Bland-Hawthorn, J. 2002, *ARA&A*, 40, 487
- [13] González Hernández, J. I., Israelian, G., Santos, N. C., et al. 2010, *ApJ*, 720, 1592
- [14] Høg, E., Fabricius, C., Makarov, V. V., et al. 2000, *A&A*, 355, L27
- [15] Kurucz, R. L. 1993, *ATLAS9 Stellar Atmosphere Programs and 2 km s⁻¹ grid*. Kurucz CD-ROM No. 13. Cambridge, Mass.: Smithsonian Astrophysical Observatory, 1993., 13,
- [16] López-Santiago, J., Montes, D., Gálvez-Ortiz, M. C., et al. 2010, *A&A*, 514, A97
- [17] van Leeuwen, F. 2007, *A&A*, 474, 653
- [18] Maldonado, J., Martínez-Arnáiz, R. M., Eiroa, C., Montes, D., & Montesinos, B. 2010, *A&A*, 521, A12
- [19] Martínez-Arnáiz, R., Maldonado, J., Montes, D., Eiroa, C., & Montesinos, B. 2010, *A&A*, 520, A79
- [20] Montes, D., López-Santiago, J., Gálvez, M. C., et al. 2001, *MNRAS*, 328, 45
- [21] Montes, D., Caballero, J. A., Fernanández-Rodríguez, C. J., et al. 2010, in *Pathways Towards Habitable Planets*, V. Coudé du Foresto, D.M. Gelino, & I. Ribas (eds.), *ASP Conf. Ser.*, 430, 507
- [22] Neves, V., Santos, N. C., Sousa, S. G., Correia, A. C. M., & Israelian, G. 2009, *A&A*, 497, 563
- [23] Paulson, D. B., Sneden, C., & Cochran, W. D. 2003, *AJ*, 125, 3185
- [24] Press, W. H., Teukolsky, S. A., Vetterling, W. T., & Flannery, B. P. 1992, Cambridge: University Press
- [25] Pompéia, L., Masseron, T., Famaey, B., et al. 2011, *MNRAS*, 415, 1138
- [26] Raskin, G., van Winckel, H., Hensberge, H., et al. 2011, *A&A*, 526, A69
- [27] Sneden, C. A. 1973, Ph.D. Thesis,
- [28] Sousa, S. G., Santos, N. C., Israelian, G., Mayor, M., & Monteiro, M. J. P. F. G. 2007, *A&A*, 469, 783
- [29] Sousa, S. G., Santos, N. C., Mayor, M., et al. 2008, *A&A*, 487, 373
- [30] Tabernero, H. M., Montes, D., & González Hernández J.I. 2012, *A&A*, 547, A13
- [31] Tabernero, H. M., González Hernández J.I., & Montes, D. 2012, in these proceedings
- [32] Tabernero, H. M., Montes, D., & González Hernández, J.I. 2012, *Cool stars* 17, AN
- [33] Tabernero, H. M., Montes, D., & González Hernández, J.I. 2012, *A&A*, in prep.